Published in final edited form as:

Phys Chem Chem Phys. 2017 January 25; 19(4): 2990–2999. doi:10.1039/c6cp07145g.

Oligomerization of FVFLM peptides and their ability to inhibit beta amyloid peptides aggregation: consideration as a possible model

M. Kouza[a,b,*], **A. Banerji**[b], **A. Kolinski**[a], **I. A. Buhimschi**[c,d,‡], and **A. Kloczkowski**[b,d,‡]

[a]Faculty of Chemistry, University of Warsaw, Pasteura 1, 02-093 Warsaw, Poland [b]Nationwide Children's Hospital, Battelle Center for Mathematical Medicine, Columbus, OH 43215 USA [c]Center for Perinatal Research, The Research Institute at Nationwide Children's Hospital, Columbus, OH 43215 USA [d]Department of Pediatrics, The Ohio State University College of Medicine, Columbus, OH 43215, USA

Abstract

Preeclampsia, a pregnancy-specific disorder, shares typical pathophysiological features with protein misfolding disorders including Alzheimer's disease. Characteristic for preeclampsia is the involvement of multiple proteins of which fragments of SERPINA1 and β-amyloid co-aggregate in urine and placenta of preeclamptic women. To explore the biophysical basis of this interaction, we investigated the multidimensional efficacy of the FVFLM sequence in SERPINA1, as a model inhibitory agent of β-amyloid aggregation. After studying the oligomerization of FVFLM peptides using all-atom molecular dynamics simulations with the GROMOS43a1 force field and explicit water, we report that FVFLM can aggregate and its aggregation is spontaneous with a remarkably faster rate than that recorded for KLVFF (aggregation "hot-spot" from β-amyloid). The fast kinetics of FVFLM aggregation was found to be driven primarily by core-like aromatic interactions originating from the anti-parallel orientation of complementarily uncharged strands. The conspicuously stable aggregation mechanism observed for FVFLM peptides is found not to conform to the popular 'dock-lock' scheme. We also found high propensity of FVFLM for KLVFF binding. When present, FVFLM disrupts the β-amyloid aggregation pathway and we propose that FVFLM-like peptides might be used to prevent the assembly of full-length Aβ or other pro-amyloidogenic peptides into amyloid fibrils

Introduction

Protein conformational disorders (also known as proteinopathies) are a growing list of diseases characterized by misfolding and aggregation of proteins[1]. Although remarkably heterogeneous with respect to primary target organs, disease manifestations and age of

* mkouza@chem.uw.edu.pl.

‡These authors contributed equally

This article is dedicated to the memory of the second author, Dr. Anirban Banerji, who passed away in Columbus, OH on Aug. 12, 2015 at the age of 39.

Electronic Supplementary Information (ESI) available: See DOI: 10.1039/x0xx00000x

onset, they are unified through a common pathogenic mechanism in which protein instability and misfolding results in the loss of normal function of the aggregated proteins along with gain of aberrant functions or toxicity driven by metastable intermediate-stage soluble oligomers. Finally, there is deposition of insoluble final-stage aggregates in adjacent tissues and organs with pathogenic consequences related to space occupying lesions[2, 3]. The most extensively studied proteinopathy is by far Alzheimer's disease and its enormous impact on individual lives, families and health systems is painfully well-known[4]. Genetic mutations or infectious-like processes resulting in protein sequences prone to aggregation and defective cellular trafficking have been implicated in diseases such as Huntington's, Parkinson's and prion disease, respectively[5]. Lastly, cancer and atherosclerosis, two of the leading causes of death in the United States have been increasingly linked to protein misfolding resulting from the interaction of genomic instability with environmental influences.

Spearheaded by proteomics research, recent experimental evidence from members of our group found that preeclampsia, a pregnancy-specific disorder, shares pathophysiological features with recognized proteinopaties[6]. Prior to our investigation there was no report of protein misfolding associated with preeclampsia[7]. While this new connection opens inroads for therapeutic intervention in preeclampsia, to devise an effective strategy we would have to draw from and if necessary broaden the knowledge gathered from a two-decade-long spectrum of studies on the numerous features of formation of linear β-sheet-rich aggregates (amyloid fibrils)[8]. Indeed, the recurrent theme of well-ordered amyloid fibrils emerging through the self-assembly of various peptides has not only been reported to be associated with numerous human medical disorders (Alzheimer's disease, prion disorders, type 2 diabetes, etc.), but also with the formation of biofilm and aerial hyphae by microorganisms[9–11]. Strikingly, the common character found in this diverse group of amyloid aggregates is manifold (predominantly β-sheet-rich conformation as a hallmark; affinity for the self-assembling Congo red dye; predictably ordered amyloid fibrils; molecular assemblies with a diameter of 7–10 nm, and a typical X-ray fiber diffraction pattern of 4.6–4.8 Å on the meridian)[12]

Alzheimer's disease is prominently characterized by aggregates of 40 to 42 residue amyloid-β (Aβ) peptides resulting from cleavage of the amyloid precursor protein (APP, a ubiquitous transmembrane glycoprotein)[13]. Devising strategies to inhibit oligomer formation of Aβ peptides has been a principal goal to fight Alzheimer's disease[14–16]; this implies either devising a strategy to block the cleaving of Aβ peptides from the aforementioned amyloid precursor protein[17] or devising an alternative strategy to inhibit the self-assembly of Aβ peptides by ensuring the presence of short peptides which may occupy the self-recognition site of a full-length Aβ peptide, thereby obstructing the aggregation of Aβ peptides[18, 19].

During our research on preeclampsia we accumulated evidence for many features of protein misfolding that overlap with those known for Aβ aggregation. These include urine congophilia with bathochromic shift, affinity for conformational state-dependent antibodies raised against aggregated Aβ peptides and dysregulation in the APP proteolytic pathway in the placenta and decidua among others[6]. Interesting for protein aggregates identified in preeclampsia was the concept of hetero-aggregation which is much less emphasized in the literature for other protein conformational disorders including Alzheimer's where the main

focus is on a single culprit protein. One particular protein, SERPINA1, caught our attention in preeclampsia. Not only fragments of SERPINA1 were part of the original urine proteomics biomarker profile but they also co-precipitated with Aβ in vivo (as plaque-like lesions in the placenta) and in vitro when Congo red was added to preeclampsia urine. Therefore, the biophysical basis of SERPINA1-Aβ interactions is significant because of the possibilities arising from hetero-aggregation. On one hand, the interactions between different proteins that promotes aggregation of one of the involved proteins are potentially very dangerous. An aggregate made up from a mixture of unrelated proteins during hetero-aggregation can be highly prone to structural polymorphism which might be associated with increased toxicity and faster disease progression[20, 21]. On the other hand, the interactions that block the binding sequences required for amyloid aggregation, but do not promote hetero-aggregation, are fascinating and important because of their potential use as protection against aggregation[19, 22].

The goal of the present paper is to report the characteristics of a novel peptide which, as found through computational investigations, demonstrates remarkable inhibition of the aggregation of Aβ peptides by being present at their self-recognition sites. With respect to the sheer pace and spontaneity of aggregation, the peptide being reported here is found to be many times superior to the commonly used peptide KLVFF[8, 19, 22]. We also report that even though intuitive and simple, the 'dock-lock' mechanism - often considered to describe the growth process to study Aβ oligomerization[23, 24], probably fails to describe the entire range of complexities observed in the aggregation of the novel peptide, as reported in this work. Furthermore, we show that a mere peptide marked by strong hydrophobic and aromatic interactions is not sufficient in efficiently blocking Aβ aggregation, and the relative orientation of the aromatic rings characterizing the peptide has been found to play a critical role in the inhibition of the self-assembly process, whereas the traditionally employed KLVFF peptide, though found to inhibit the Aβ oligomerization, could be noted to be not as superior as an oligomerization-blocker as the novel FVFLM peptide. A description and in-depth explanation of the facets of the FVFLM peptide’s better efficiency as an oligomerization-blocking agent as compared to that recorded for KLVFF, with discussion of the ramifications of these findings in the general context of multifarious future studies on the inhibition of self-assembly of Aβ peptides, forms the subject matter of this work.

We proposed undertaking a systematic examination of protein misfolding to combat PE-disorders during our earlier proteomics study in which we found that women with PE excrete a panel of non-random fragments of SERPINA1 and albumin. We further reported that the presence of fragments corresponding to 21 and 22 amino acid C-terminus sequences was found to be associated with high confidence with clinically severe diseases[25]. While the detailed account of the physical chemistry of these two fragments was provided in our previous papers (as well as in Fig. S1 in SM), it suffices for the present work to note that we deduced that the two cleavages that generate the aforementioned fragments occurred within a stretch of five hydrophobic amino acids (381FVF↓L↓M385, with ↓ indicating the cleavage sites). It is noted that this site is the recognition sequence for the hepatic serpin-enzyme complex (SEC) receptor which removes circulating SERPINA1-enzyme complexes[26], and to investigate the biophysical nature of the five residue FVFLM peptide and its efficiency and reliability as a binding agent, we attempt here to answer the following questions:

Can the FVFLM peptide be considered a reliable model aggregating system to investigate the C-terminal sequence fragments found in the excretions of preeclampsia patients?

How completely does the presence of FVFLM disrupt the $A\beta_{16–20}$ aggregation pathway?

Can the FVFLM peptide be considered to consistently prevent the assembly of full-length Aβ into amyloid fibrils?

We start by noting that in several previous works[18, 19, 27, 28] $A\beta_{16–20}$ (KLVFF) or short LPFDD peptides have been shown to occupy the self-recognition site of the full length Aβ-peptide interfering with the aggregation process. In this backdrop of knowledge base, upon observing the pivotal importance of the five hydrophobic residue FVFLM peptide in influencing cleavage in PE excretion fragments (see above), we pursued two related generalized questions:

Could even more effective inhibitors exist compared to the known KLVFF (and LPFDD)?

and

Could, and if so, to what extent, the FVFLM peptide function as a more efficient and more consistent inhibitor than the commonly employed ones?

To address these questions and those posed before, we studied the self-assembly of the FVFLM peptide and its influence on the kinetics of $A\beta_{16–20}$ oligomerization using all-atom simulation with the GROMOS43a1 force field in explicit solvent. We found that the population in the fibril-prone conformation of the FVFLM monomer was much higher than the KLVFF population. The fibril formation time of FVFLM peptides was found to be notably faster than for KLVFF. The observation of faster (and spontaneous) aggregation rates of FVFLM found support in the distinctly downhill picture of the free energy landscape of FVFLM. In contrast, the free energy landscape of KLVFF suggested that to arrive at the fibril-prone conformations numerous energy barriers must be overcome. In addition, we demonstrated that the Aβ fibril growth process was significantly hampered in the presence of the FVFLM peptide. Alongside, we report that the increased probability of aromatic interactions is an influential factor governing oligomer formation rates and it possibly contributes to the stability of oligomers.

As stated before, because the present work originated primarily from the need to provide a theoretically robust explanation for the observations made in our wet-lab experiments[6], a summary of those wet-lab findings may help the readers equipped with knowledge of those intricate details. However, because such details are not necessary to appreciate the theoretical explanation provided here, an outline of the pertinent wet-lab findings is provided in Supplementary Material-1.

Model and Methods

We used the GROMOS43a1[29] force-field[30] to describe the peptides and the SPC[31] water model for solvent. All-atom MD simulations were carried out using the Gromacs program

suite[32] which was previously successfully employed by our group in studying protein folding[33], unfolding[34] and aggregation[35]. We use periodic boundary conditions and calculate electrostatic interactions by the particle mesh Ewald method[36]. Non-bonded interaction pair-lists are updated every 10 fs, using a cutoff of 1.5 nm. All bond lengths are constrained with the linear constraint solver LINCS[37] allowing us to integrate the equations of motion with a time step of 2 fs.

The initial configuration of dimers and trimers was obtained by replicating randomly the monomers in random orientations and putting them in space far enough that no intermolecular contacts were present. The monomers were placed in a dodecahedral box of such a size that the minimal distance between the monomer and the box was 1.5 nm. This was followed by solvation with 815–7102 water molecules. A small number of water molecules were used for monomers, while a larger number of water particles were required for the dimer and trimer. To avoid improper structures, the whole system was minimized with the steepest-descent method, before being equilibrated at 300 K with two successive molecular dynamics runs of 1 ns each; the first one at constant volume, and the second at constant pressure (1atm). Initial velocities of the atoms were generated from the Maxwell distribution at 300 K. Temperature was kept close to 300K using a v-rescale thermostat. Data analysis was done using corresponding Gromacs programs and snapshots of all peptides were created with VMD software[38].

Probability of fibril-prone conformation in the monomeric state

Fibril-prone conformations of the peptide were identified upon measuring the end-to-end distance, R, between the first and last alpha-carbon atoms of the monomer. Employing a strict criterion, in cases where R exceeded 90% of R_{max} (with R_{max} being the end-to-end distance of a fully-extended peptide), the fibril-prone conformations were identified.

Contact maps

We monitored the time evolution of the formation of the side chain-side chain (Cβ-Cβ) contacts and the hydrogen bond (HB) contacts. An SC-SC contact was considered to be formed if the distance between the centers of mass of two Cβ residues was found to be ≤6.0Å. An HB contact was considered provided that the distance between donor D and acceptor A was found to be ≤3.5Å and the angle D-H-A was found to be ≥135°.

Free-energy landscape

The two-dimensional free-energy landscape surface, constructed along the radius of gyration (R_g) as one axis and the end-to-end distance (R), as the other, was given by $\Delta G(R_g,R) = -k_B T[\ln P(R_g,R) - \ln P_{max}]\Delta G(R_g,R)=-k_B T[\ln P(R_g,R)-\ln P_{max}]$, where $P(R_g,R)$ P(R$_g$,R)was the probability distribution obtained from a histogram of MD data. $P_{max}P_{max}$ was subtracted to ensure ΔG=0 at the global minimum of free-energy.

Median time for dimerization

The dimerization time is defined as the first passage time to reach an antiparallel ordered structure (with 3 or more backbone HBs between monomers) starting from random monomers. The median time serves as an estimate of dimerization time for the studied

systems if the fibril state is not observed in all studied trajectories. As we have 8 trajectories for each system, the median time is defined as the mean of the 4th and 5th values.

Results and Discussions

Computational predictions of FVFLM aggregation propensity

We started our investigation by screening proteins and peptides found in the urine of pregnant women diagnosed with the PE disease. Predictions from available web-servers such as Aggrescan[39], Fold-amyloid[40], Zyggregator[41], GOR[42] suggested unambiguously that the short peptide FVFLM of SERPINA protein is highly amyloidogenic. In particular, Zyggregator predicted at pH=7.0 higher aggregation propensity Z^{agg}=2.512 for FVFLM than Z^{agg}=1.922 for KLVFF (aggregation "hot-spot" from β-amyloid), indicating that FVFLM peptides have higher propensity to aggregate than KLVFF peptides. Mutation experiments[43] as well as coarse-grained simulations[44] provided evidence that the increase in hydrophobicity accelerates fibril elongation. It should be noted that even a 5% difference in sequence similarity between $A\beta_{1-40}$ and $A\beta_{1-42}$ could lead to a difference in oligomerization pathways[45] and their toxicity. We also noted that Bitan et al. showed that the distribution of the hydrophobic residues plays an important role in protein oligomerization[46]. In this context we observed that the popularly employed KLVFF peptide is comprised of four hydrophobic amino acids and one hydrophilic Lys, which summed up the total charge of the monomer to be −1. The FVFLM from SERPINA, on the other hand, contains Met instead of Lys, making it more hydrophobic than KLVFF. Based on the hydrophobicity of individual amino acids, faster aggregation of FVFLM relative to KLVFF was expected. Therefore, through MD simulation we proposed to examine how the ability of FVFLM peptides cooperates at the atomistic level for self-assembly and how it acquires its inhibition potency of β-amyloid oligomerization.

The population of fibril-prone conformations in the monomeric state of KLVFF is lower than FVFLM

Given the possibly superior aggregation propensity obtained through our preliminary assessment (see above), we focused on a thorough comparative investigation of the aggregation propensity of FVFLM and KLVFF monomers. Upon performing a rigorous set of analyses, we had proposed in one of our recent works[47] that oligomer formation times are strongly correlated with the population of the fibril-prone conformation in the monomeric state[47]. The larger the population of fibril-prone conformations in the monomeric state, the faster we demonstrated its aggregation process would be. The result of our investigation in the present context of comparative analysis is presented in Fig. 1 which shows the end-to-end distance, R, as a function of time for FVFLM and KLVFF peptides. We defined the fibril-prone conformation as one with R exceeding 90% of the fully extended conformation. Using this criterion, we noted the population of peptides in the fibril-prone state to be 21.05% and 13.07% for FVFLM and KLVFF, respectively.

In the absence of a consensus on the definition of the fibril-prone state, we also calculated the population of peptides in the fibril state if R exceeded 80% of the fully extended conformation (yellow line in Fig. 1). Strikingly, at the 80% threshold, the difference between

cases was found to be nearly two-fold. This finding demonstrated that FVFLM is more ordered in the monomeric state than KLVFF, a finding which may provide a basis, though qualitative, behind FVFLM's comparative superiority in preliminarily predicted aggregation propensity. Because the population of fibril prone conformations is required for oligomerization to begin, our result implies that the propensity of FVFLM for self-assembly is higher than for KLVFF.

Stability of KLVFF and FVFLM monomers

To compare the stability of KLVFF and FVFLM peptides we analyzed the free-energy landscape profiles of KLVFF and FVFLM as a function of the end-to-end distance (R) and radius of gyration (Rg), as shown in Fig. 2. The free-energy landscape surface of KLVFF reveals three minima separated by energy barriers of 0.5–1.5 kBT. A local minimum 1 was found to be located at small values of R and Rg (4.5, 4.6) corresponding to compact U-shape conformations, stabilized by N- and C-terminal interactions. A local minimum 3 represented extended conformations with large values of R. The most populated minimum 2 was found to be centered at coordinates (10, 4.8) representing a pre-extended configuration, less compact than the U-shape. The typical snapshots of representative conformations are shown in Fig. 2c. However, it is worth observing that despite the 3-state free energy landscape, the monomeric state of KLVFF is not stable, because the minima (0.5–1.5 kBT) are found to be separated by stiff free energy barriers between them. The result that the KLVFF native state has low stability is consistent with the hypothesis that instability of the native state is one of the factors which facilitate oligomerization[44, 48, 49]. Based on a recently proposed mathematical framework to investigate macroscopic emergence[50], we attempted to derive mathematically how KLVFF's ability to ensure peptide aggregation can be explained as its macroscopically emergent property by building upon the innate instability of KLVFF monomers. However, such a formal framework could not be established as it did not meet the statistically significant number of some of the parameters derived from the five-residue peptide.

In contrast, the free energy landscape of FVFLM (Fig. 2b) was found to contain just one broad minimum, which was found to be mainly populated by extended conformations with large values of R. The (almost) monotonically downhill nature of the free energy landscape implied clearly that fibril-prone conformations of FVFLM are much easily accessible, compared to those for the KLVFF peptide. This explained why the FVFLM fibril formation rates were observed to be faster compared to those observed for the KLVFF peptide.

Oligomerization of FVFLM peptides. Antiparallel ordering

To investigate FVFLM fibrillation capacity we performed eight molecular dynamics runs starting from its random configurations. The goal was to investigate the formation of simplest aggregation units such as dimers and trimers which mimic the β-sheet conformations found in the fibril state. Fig. 3 shows the time dependence of the number of backbone hydrogen bonds between monomers. Defining the dimerization time as the time needed to form at least 3 backbone hydrogen bonds between monomers, we estimated the averaged time needed to form a dimer. Averaging this time over eight trajectories we obtained the mean FVFLM dimerization time, $\tau_{dimer}^{FVFLM} \approx 17$ ns which was slightly

lower than that for KLVFF, $\tau_{dimer}^{KLVFF} \approx 23$ ns (Fig. S2). In addition, we observed FVFLM trimer formation in all simulations, except for the case of trajectory 4. We estimated the median time for trimer formation, $\tau_{trimer}^{FVFLM} \approx 51.4$ ns, found to be significantly smaller than $\tau_{trimer}^{KLVFFAE} \approx 244$ ns, as was previously reported for the $A\beta_{16–22}$ association[23]. We detected KLVFF trimer formation in 4 out of 8 trajectories (Fig. S2). However, because we stopped all simulations at 100ns, the 5th value of trimerization time for KLVFF would be greater than 100 ns. Based on this, we could presume that the median time of $A\beta_{16–20}$ trimer formation is slightly greater than 100 ns. Analyses presented in this section thus revealed that the formation time of dimers and trimers of FVFLM monomers was much faster than for $A\beta_{16–20}$ (KLVFF) and $A\beta_{16–22}$ (KLVFFAE) sequences.

As seen from Fig. 3 for all trajectories we observed antiparallel β-sheet structures only. But the oligomerization pathways were clearly diverse. This is a notable finding because it is known that different starting configurations lead to antiparallel β-sheet structures via very different routes. The dimers are formed relatively fast in all trajectories. A “typical” pathway was observed in Trajectories 1, 2, 3, 5, 6 and 7, where dimer formation was observed to be followed by the formation of a trimer. Conspicuously, for trajectory 8 the dimer of P1 and P2 was found to form transiently very fast, but then this state was not stable, whereby the dimer was found to dissociate and after only 50 ns dimerization reoccurred, but in this case involving P2 and P3 (and not involving P1 and P2 as observed in an earlier time-point of the same trajectory). Three different dimers were formed in Trajectory 4 and dimer states were found to be quite stable (for tens of ns), though trimer formation could not be observed for this trajectory. It is important to note that generally the association of FVFLM monomers was observed to take place in a cooperative manner, because the scheme of cooperative association disagrees with the scheme of previously proposed 'dock-lock' explanation of β-amyloid formation. The popular scheme to explain the mechanism of β-amyloid fibrillation, the 'dock-lock' hypothesis[23], predicts a fast stage of docking between a nascent peptide and a preformed template, followed by a significant time that the peptide needs to be locked to the preformed template of peptides. Instead, Fig. 3 demonstrates that the transition to the ordered β-sheet structure occurs very fast (almost spontaneously) without repeatedly sampling configurations with 1 or 2 HBs, which has been known to be the signature of the locking stage. We did not observe long-lived intermediates. The relatively short lock stage in FVFLM aggregation was observed to lead to a faster aggregation rate of FVFLM self-assembly, compared to that of β-amyloid peptides.

Oligomerization of KLVFF peptides. Antiparallel ordering

Many reports are available on the self-assembly of β-sheet-forming peptides, and they often note commonality among a diverse array of cases. However, we note that there is controversy regarding the self-assembly process of KLVFF peptides. Although the KLVFF motif is known to be the critical sequence for fibrillization[51–53], Tjernberg et al.[54] reported that the KLVFF fragment could not form fibrils. On the other hand, transmission electron microscopy studies indicated that KLVFF itself formed fibrils in aqueous phosphate-buffered saline solutions (pH=7.4)[28]. In this work we made an attempt to examine this problem by resorting to thorough analyses through MD simulations.

Our data suggest that KLVFF, like its parent KLVFFAE, is capable of forming oligomers. We observed the dimerization of the KLVFF monomers in all eight trajectories, among them trimer formation was observed in 4 trajectories (Fig. S2). Though the trajectories were quite diverse, we could estimate (albeit roughly) that the median time needed to form a KLVFF trimer was slightly greater than 100 ns. This, we noted, was significantly shorter than 244 ns reported for the association of three $A\beta_{16–22}$ peptides[23]. Thus, our work demonstrates that the short KLVFF peptide can undergo self-assembly and its kinetics is faster compared to $A\beta_{16–22}$.

We then attempted to decipher the driving force behind the fast KLVFF oligomerization. It is commonly believed that one of the main driving forces of KLVFFAE ($A\beta_{16–22}$) organization and stability are electrostatic interactions[55]. Although the prominent role of electrostatic interactions in the anti-parallel ordering of $A\beta_{16–22}$ between positively charged C-terminal Lys and negatively charged C-terminal Glu has been pointed out many times[23, 56], our results that KLVFF peptides can self-assemble (Fig. S2 in SM) suggest that such a popularly accepted proposal falls short of capturing the entire complexity of the process.

Simulations of KLVFF assembly demonstrated that even without the presence of the negatively charged C-terminus, the anti-parallel ordering could still remain favorable. Moreover, the anti-parallel ordering was also found to be favorable for FVFLM peptides (which are completely hydrophobic) with very fast aggregation rates. These findings suggested that previous simulations, banking on calculation of isotropic electrostatics, might have overestimated the role of electrostatic interactions in the aggregation and stability of β-amyloid peptides. Based on the present set of results we note that to probe the systemic physicochemical aspects of the aggregation mechanism, it will be important to ascertain whether the loss of electrostatic interactions can be compensated by hydrophobic or dispersion or stacking interactions. Examination of peptide variants in which one of the charged residues of $A\beta_{16–22}$ is replaced either by a hydrophobic residue Ile (Leu) or Phe which has comparable hydrophobicity to Ile (Leu) but is also capable of aromatic interactions (π-stacking) can probe the role of hydrophobic and aromatic interactions in the peptide aggregation process. We are presently testing this idea, although it does not form a part of the current paper.

Arrest of KLVFF ($A\beta_{16–20}$) aggregation by the FVFLM peptide

To address the question whether FVFLM can associate with KLVFF peptides, we performed eight MD runs in which one FVFLM peptide was injected into the system with two $A\beta_{16–20}$ peptides. As before, we started from random conformations and monitored the kinetics of monomer association. Rapid dimer formation between FVFLM and one of $A\beta_{16–20}$ peptides could be consistently observed for all the eight trajectories (Fig. 4). Interestingly, the dimerization of FVFLM and KLVFF was found to be followed by trimer formation for Trajectory 4, 6 and 8 (e.g., binding of another $A\beta_{16–20}$ peptide to FVFLM). Trimer formation was observed in Trajectory 7 too, but we found that this was a solitary trajectory where the dimerization of KLVFF peptides occurred. The fast kinetics of FVFLM binding to KLVFF suggests that FVFLM may be capable of binding the KLVFF-sequence of beta-amyloid. The KLVFF peptide is critical for binding to $A\beta_{1–42}$ and blocking the KLVFF

binding sequence of beta amyloid required for amyloid aggregation has been shown to interfere with beta amyloid fibrillation.[18, 19, 52, 53]. We propose to use FVFLM as recognition sequence to interact not only with SERPINA1, the parent protein of peptides aggregated in preeclampsia, but also with KLVFF sequence of $A\beta_{1–42}$ especially since preeclampsia aggregates were demonstrated to include both SERPINA1 and Aβ immunoreactivity[6] The scope and discernible trends in Fig. 4 suggest unambiguously that the presence of the FVFLM peptide interacts precipitously with β-amyloid aggregation hot-spot (KLVFF) formation, whereby we propose its use as a potent inhibitor of β-amyloid oligomerization.

Mapping of interpeptide interactions. Importance of aromatic interactions

Several reports over the last decade have attempted to identify the canonical set of dominating interactions shaping protein (and peptide) self-assembly[23, 57]. To answer the question of what is behind the different self-assembly rates and what interactions critically influence oligomer stabilization, we calculated the contacts formed between monomer side-chains and main-chain hydrogen bonds. It was already shown that side-chain interactions may influence amyloid fibril formation[58] (*e.g.*, the APS23TYR mutation of $A\beta_{10–40}$ eliminated the strong side-chain interactions in the wild type protein and promoted oligomerization growth). We argue, based on the present results, that our findings also support the conjecture of positive influence of side-chain interactions on amyloid formation. As evident from Fig. 4, FVFLM monomers were found to form about ~10% more interpeptide side-chain contacts than KLVFF monomers. The probability of backbone hydrogen bond formation between FVFLM monomers was ~8% higher than for KLVFF monomers (data not shown). We argue that in general an increased possibility of side-chain contacts and hydrogen bond formation affects aggregation kinetics and enhances the stability of a β-sheet formed by FVFLM monomers.

In contrast to the nonspecific hydrophobic (and at times, dispersion) interactions, the significance of aromatic interactions in imparting a particular pattern of molecular interactions leading to the formation of ordered amyloid structure has been suggested for some time[59, 60]. The results obtained in the present investigation bolstered such a hypothesis, especially to categorically assess the advantage of FVFLM over KLVFF as the choice of an aggregating peptide. A higher probability of forming Phe-Phe contacts, as observed for the FVFLM peptide in contrast to KLVFF, provides a possible explanation behind the observation of faster kinetics and stable aggregation of the former (Fig. 5 and Fig. 6). In addition to hydrophobic interactions, the interactions between aromatic rings are known to lend extra contribution to oligomer stability. Aromatic-aromatic interactions were known to be involved in protein stabilization[61], contributing ~ −1 kcal/mol to their structural stability[62], and they were observed to be larger than the distances between donor and acceptor atoms involved in hydrogen bond interactions; therefore, we postulated their likely mediation in the formation of side chain contacts and hydrogen bonds. This provides a reasonable explanation for observing faster kinetics of fibril formation for FVFLM peptides than for KLVFF peptides. Upon noticing an unmistakable similarity between the problem in the present investigation and that in a set of previous reports[19, 63–65] about the singularly influential role of Phe positioning and conformation, we hypothesized that the difference in

observed fibril formation times between KLVFF and FVFLM may be attributed to the different positioning of Phe's along the peptide sequence alongside the side-chain conformations of these. Unlike in KLVFF where Phe side chains were found to stick out in opposite directions, positions of Phe residues in the FVFLM sequence were found to allow the formation of a network of three or more interacting aromatic side chains. We may thus infer that the fast association of FVFLM peptides was promoted by an increased possibility of Phe-Phe interactions, supporting the existing belief that together with intrinsic and environmental properties, the aromatic interactions are crucial determinants governing fibril formation rates[59, 66, 67].

Robustness of results against potential sampling bias

So far we have carried out eight MD trajectories for each system. In order to check the robustness of our results, we performed the additional set of eight 100 ns MD runs for FVFLM system. Within 100 ns in all trajectories we observed dimers and trimers which mimic the β-sheet conformations found in the fibril state (See Fig. S3 in Supplementary Material). Combining data from two sets and calculating the median time over 16 trajectories as the mean of 8th and 9th values, we obtained $\tau_{trimer}^{FVFLM} \approx 46$ ns. This value is smaller than $\tau_{trimer}^{KLVFF} \approx 100$ ns obtained for KLVFF and it is comparable to the median time $\tau_{trimer}^{FVFLM} \approx 51.4$ ns obtained from the first eight trajectories for FVFLM system. Thus we conclude that the difference in fibril formation rates of FVFLM and KLVFF peptides is robust against data sampling and we expect it to hold for larger number of trajectories. Given Fig. S3, we observe that the association of FVFLM monomers takes place in a cooperative manner without significant sampling of the locking stage. Taken together, the overall picture about aggregation rates and pathway kinetics remains the same as in the case of 8 trajectories supporting FVFLM's distinct ability to form fast oligomers.

Conclusions

Acknowledging the sheer importance of a thorough comparative investigation into multiple aspects of oligomer formation of the popular "model system" (the KLVFF peptide) against the FVFLM peptide identified previously through experimental works by our group, we undertook a rigorous and extensive set of studies. Employing all-atom models with explicit solvent, we investigated aggregation rates of short KLVFF and FVFLM peptides and from multiple perspectives established the comparative benefits of using FVFLM over KLVFF as the "model system" to be used in aggregation studies of myriad types.

We have presented molecular dynamics simulations that confirm the ability of KLVFF and FVFLM peptides to aggregate. More importantly, the results of this study demonstrated that FVFLM form antiparallel β-sheet oligomers faster than KLVFF. The fast kinetics of FVFLM was driven by hydrophobic and aromatic interactions. If FVFLM is injected into the system with two KLVFF ($A\beta_{16–20}$) peptides, it was found to arrest one of the KLVFF peptides thus reducing the propensity of KLVFF self-assembly.

Our computational result demonstrating FVFLM's distinct ability to form fast and stable oligomers supports results of recent experiments[6] with urine of pregnant women with preeclampsia. Since the structure of preeclampsia-related oligomers has not yet been solved,

we predict that FVFLM, either by itself or together with other proteins, is a strong candidate to be one of the major components of potentially toxic preeclampsia aggregates. However, the stoichiometry between the level of aggregation of FVFLM and aggregate toxicity remains to be determined. It is important to consider the possibility that FVFLM's aggregation is consequent to the suicide inhibition mechanism characterizing SERPINA-1 antiproteolytic activity. Therefore, modulating the cleavage of SERPINA1 or the self-assembly of FVFLM peptides may be a strategy for preeclampsia prevention.

Supplementary Material

Refer to Web version on PubMed Central for supplementary material.

Acknowledgments

A. Kol. and M. K. would like to acknowledge support from the National Science Center grant [MAESTRO 2014/14/A/ST6/00088]. M.K. acknowledges the Polish Ministry of Science and Higher Education for financial support through “Mobilność Plus” Program No. 1287/MOB/IV/2015/0. A. Klo. acknowledges support by the NSF grant MCB-1021785 and National Institutes of Health grant R01GM072014, and the start-up funds from The Research Institute at Nationwide Children’s Hospital. IAB acknowledges support from the Eunice Kennedy Shriver National Institute of Child Health and Human Development (NICHD) R01HD084628 and The Research Institute at Nationwide Children’s Hospital's John E. Fisher Endowed Chair for Neonatal and Perinatal Research.

Notes and references

1. Winklhofer KF, Tatzelt J, Haass C. EMBO J. 2008; 27:336–349. [PubMed: 18216876]
2. Glabe CG. Journal of Biological Chemistry. 2008; 283:29639–29643. [PubMed: 18723507]
3. Hipp MS, Park SH, Hartl FU. Trends in Cell Biology. 2014; 24:506–514. [PubMed: 24946960]
4. Selkoe DJ. Physiological Reviews. 2001; 81:741–766. [PubMed: 11274343]
5. Moreno-Gonzalez I, Soto C. Seminars in Cell & Developmental Biology. 2011; 22:482–487. [PubMed: 21571086]
6. Buhimschi IA, Nayeri UA, Zhao G, Shook LL, Pensalfini A, Funai EF, Bernstein IM, Glabe CG, Buhimschi CS. Sci Transl Med. 2014; 6:245ra292.
7. Pennington KA, Schlitt JM, Jackson DL, Schulz LC, Schust DJ. Disease Models & Mechanisms. 2012; 5:9–18. [PubMed: 22228789]
8. Lowe TL, Strzelec A, Kiessling LL, Murphy RM. Biochemistry. 2001; 40:7882–7889. [PubMed: 11425316]
9. Chapman MR, Robinson LS, Pinkner JS, Roth R, Heuser J, Hammar M, Normark S, Hultgren SJ. Science. 2002; 295:851–855. [PubMed: 11823641]
10. Claessen D, Rink R, de Jong W, Siebring J, de Vreugd P, Boersma FGH, Dijkhuizen L, Wosten HAB. Genes & Development. 2003; 17:1714–1726. [PubMed: 12832396]
11. Gebbink MFBG, Claessen D, Bouma B, Dijkhuizen L, Wosten HAB. Nature Reviews Microbiology. 2005; 3:333–341. [PubMed: 15806095]
12. Serpell LC. Bba-Mol Basis Dis. 2000; 1502:16–30.
13. Selkoe DJ. Nature Cell Biology. 2004; 6:1054–1061. [PubMed: 15516999]
14. Yan LM, Velkova A, Tatarek-Nossol M, Andreetto E, Kapurniotu A. Angewandte Chemie-International Edition. 2007; 46:1246–1252. [PubMed: 17203498]
15. Frydman-Marom A, Rechter M, Shefler I, Bram Y, Shalev DE, Gazit E. Angew Chem Int Ed Engl. 2009; 48:1981–1986. [PubMed: 19035593]
16. Nasica-Labouze J, Nguyen PH, Sterpone F, Berthoumieu O, Buchete NV, Cote S, De Simone A, Doig AJ, Faller P, Garcia A, Laio A, Li MS, Melchionna S, Mousseau N, Mu YG, Paravastu A, Pasquali S, Rosenman DJ, Strodel B, Tarus B, Viles JH, Zhang T, Wang CY, Derreumaux P. Chemical Reviews. 2015; 115:3518–3563. [PubMed: 25789869]

17. Citron M. Nature Reviews Neuroscience. 2004; 5:677–685. [PubMed: 15322526]
18. Chafekar SM, Malda H, Merkx M, Meijer EW, Viertl D, Lashuel HA, Baas F, Scheper W. Chembiochem. 2007; 8:1857–1864. [PubMed: 17763487]
19. Tjernberg LO, Naslund J, Lindqvist F, Johansson J, Karlstrom AR, Thyberg J, Terenius L, Nordstedt C. Journal of Biological Chemistry. 1996; 271:8545–8548. [PubMed: 8621479]
20. Miller Y, Ma B, Nussinov R. Chemical Reviews. 2010; 110:4820–4838. [PubMed: 20402519]
21. Fandrich M, Meinhardt J, Grigorieff N. Prion. 2009; 3:89–93. [PubMed: 19597329]
22. Kumaraswamy P, Sethuraman S, Krishnan UM. Rsc Advances. 2015; 5:59480–59490.
23. Nguyen PH, Li MS, Stock G, Straub JE, Thirumalai D. Proceedings of the National Academy of Sciences of the United States of America. 2007; 104:111–116. [PubMed: 17190811]
24. Straub JE, Thirumalai D. Annu Rev Phys Chem. 2011; 62:437–463. [PubMed: 21219143]
25. Buhimschi IA, Zhao GM, Funai EF, Harris N, Sasson IE, Bernstein IM, Saade GR, Buhimschi CS. American Journal of Obstetrics and Gynecology. 2008; 199
26. Joslin G, Fallon RJ, Bullock J, Adams SP, Perlmutter DH. Journal of Biological Chemistry. 1991; 266:11282–11288. [PubMed: 1645729]
27. Viet MH, Ngo ST, Lam NS, Li MS. Journal of Physical Chemistry B. 2011; 115:7433–7446.
28. Gordon DJ, Tappe R, Meredith SC. Journal of Peptide Research. 2002; 60:37–55. [PubMed: 12081625]
29. Scott WRP, Hunenberger PH, Tironi IG, Mark AE, Billeter SR, Fennen J, Torda AE, Huber T, Kruger P, van Gunsteren WF. Journal of Physical Chemistry A. 1999; 103:3596–3607.
30. Cornell WD, Cieplak P, Bayly CI, Gould IR, Merz KM, Ferguson DM, Spellmeyer DC, Fox T, Caldwell JW, Kollman PA. Journal of the American Chemical Society. 1996; 118:2309–2309.
31. Berendsen HJC, M PJP, van Gunsteren WF, J H. Intermolecular Forces. 1981; 14:331–442.
32. Hess B, Kutzner C, van der Spoel D, Lindahl E. Journal of Chemical Theory and Computation. 2008; 4:435–447. [PubMed: 26620784]
33. Kouza M, Hansmann UHE. Journal of Physical Chemistry B. 2012; 116:6645–6653.
34. Kouza M, Hu CK, Zung H, Li MS. Journal of Chemical Physics. 2009; 131
35. Kouza M, Co NT, Nguyen PH, Kolinski A, Li MS. J Chem Phys. 2015; 142:145104. [PubMed: 25877597]
36. Darden T, York D, Pedersen L. Journal of Chemical Physics. 1993; 98:10089–10092.
37. Hess B, Bekker H, Berendsen HJC, Fraaije JGEM. Journal of Computational Chemistry. 1997; 18:1463–1472.
38. Humphrey W, Dalke A, Schulten K. Journal of Molecular Graphics & Modelling. 1996; 14:33–38.
39. Castillo V, Grana-Montes R, Sabate R, Ventura S. Biotechnology Journal. 2011; 6:674–685. [PubMed: 21538897]
40. Garbuzynskiy SO, Lobanov MY, Galzitskaya OV. Bioinformatics. 2010; 26:326–332. [PubMed: 20019059]
41. Tartaglia GG, Vendruscolo M. Chemical Society Reviews. 2008; 37:1395–1401. [PubMed: 18568165]
42. Kouza, M., Faraggi, E., Kolinski, A., Kloczkowski, A. Prediction of Protein Secondary Structure. Zhou, Y.Kloczkowski, A.Faraggi, E., Yang, Y., editors. Vol. 1484. New York: Humana Press; 2017. p. 7-24.
43. Chiti F, Stefani M, Taddei N, Ramponi G, Dobson CM. Nature. 2003; 424:805–808. [PubMed: 12917692]
44. Li MS, Co NT, Reddy G, Hu CK, Straub JE, Thirumalai D. Physical Review Letters. 2010; 105
45. Bitan G, Kirkitadze MD, Lomakin A, Vollers SS, Benedek GB, Teplow DB. Proceedings of the National Academy of Sciences of the United States of America. 2003; 100:330–335. [PubMed: 12506200]
46. Xiong HY, Buckwalter BL, Shieh HM, Hecht MH. Proceedings of the National Academy of Sciences of the United States of America. 1995; 92:6349–6353. [PubMed: 7603994]
47. Nam HB, Kouza M, Hoang Z, Li MS. Journal of Chemical Physics. 2010; 132
48. Chiti F, Dobson CM. Annual Review of Biochemistry. 2006; 75:333–366.

49. Zhuravlev PI, Reddy G, Straub JE, Thirumalai D. Journal of Molecular Biology. 2014; 426:2653–2666. [PubMed: 24846645]
50. Banerji A, Ghosh I. Journal of Mathematical Chemistry. 2011; 49:643–665.
51. Hamley IW. Angewandte Chemie-International Edition. 2007; 46:8128–8147. [PubMed: 17935097]
52. Tjernberg LO, Lilliehook C, Callaway DJE, Naslund J, Hahne S, Thyberg J, Terenius L, Nordstedt C. Journal of Biological Chemistry. 1997; 272:17894–17894.
53. Rojas AV, Liwo A, Scheraga HA. J Phys Chem B. 2011; 115:12978–12983. [PubMed: 21939202]
54. Tjernberg LO, Callaway DJE, Tjernberg A, Hahne S, Lilliehook C, Terenius L, Thyberg J, Nordstedt C. Journal of Biological Chemistry. 1999; 274:12619–12625. [PubMed: 10212241]
55. Ma BY, Nussinov R. Proceedings of the National Academy of Sciences of the United States of America. 2002; 99:14126–14131. [PubMed: 12391326]
56. Berhanu WM, Hansmann UHE. Protein Science. 2012; 21:1837–1848. [PubMed: 23015407]
57. Klimov DK, Thirumalai D. Structure. 2003; 11:295–307. [PubMed: 12623017]
58. Takeda T, Klimov DK. Journal of Physical Chemistry B. 2009; 113:11848–11857.
59. Gazit E. Faseb Journal. 2002; 16:77–83. [PubMed: 11772939]
60. Galzitskaya OV, Garbuzynskiy SO, Lobanov MY. Plos Computational Biology. 2006; 2:1639–1648.
61. Burley SK, Petsko GA. Science. 1985; 229:23–28. [PubMed: 3892686]
62. Serrano L, Bycroft M, Fersht AR. Journal of Molecular Biology. 1991; 218:465–475. [PubMed: 2010920]
63. Findeis MA, Musso GM, Arico-Muendel CC, Benjamin HW, Hundal AM, Lee JJ, Chin J, Kelley M, Wakefield J, Hayward NJ, Molineaux SM. Biochemistry. 1999; 38:6791–6800. [PubMed: 10346900]
64. Soto C, Sigurdsson EM, Morelli L, Kumar RA, Castano EM, Frangione B. Nature Medicine. 1998; 4:822–826.
65. Balbach JJ, Ishii Y, Antzutkin ON, Leapman RD, Rizzo NW, Dyda F, Reed J, Tycko R. Biochemistry. 2000; 39:13748–13759. [PubMed: 11076514]
66. Porat Y, Abramowitz A, Gazit E. Chemical Biology & Drug Design. 2006; 67:27–37. [PubMed: 16492146]
67. Tartaglia GG, Cavalli A, Pellarin R, Caflisch A. Protein Science. 2004; 13:1939–1941. [PubMed: 15169952]

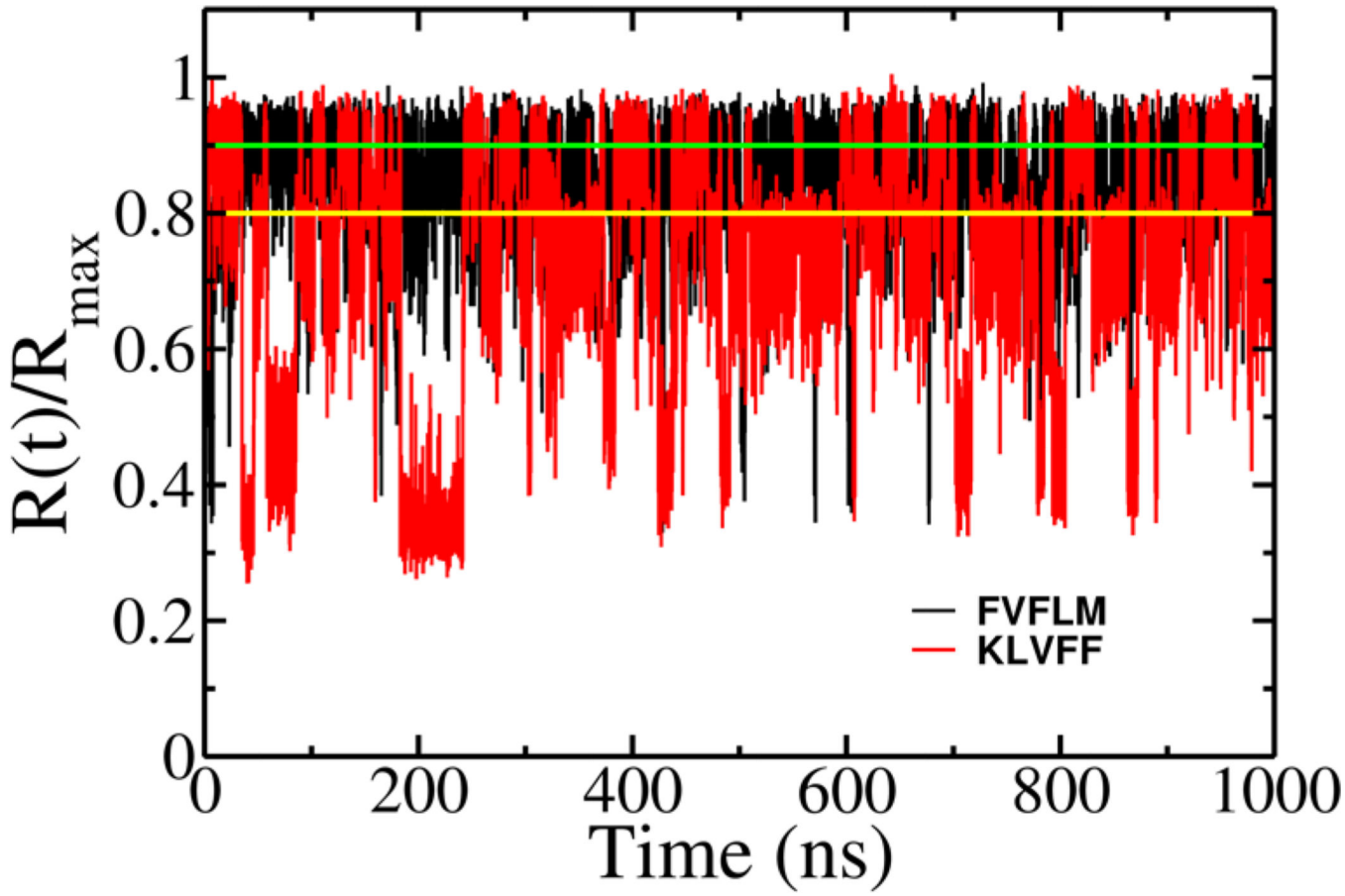

Figure 1.

Time dependence of the end-to-end distance renormalized by Rmax for FVFLM and KLVFF monomers. Results are averaged in a 40ps window. Rmax = 1.426 nm is the maximumend-to-end distance obtained in simulations. The green and yellow lines refer to R/Rmax=0.

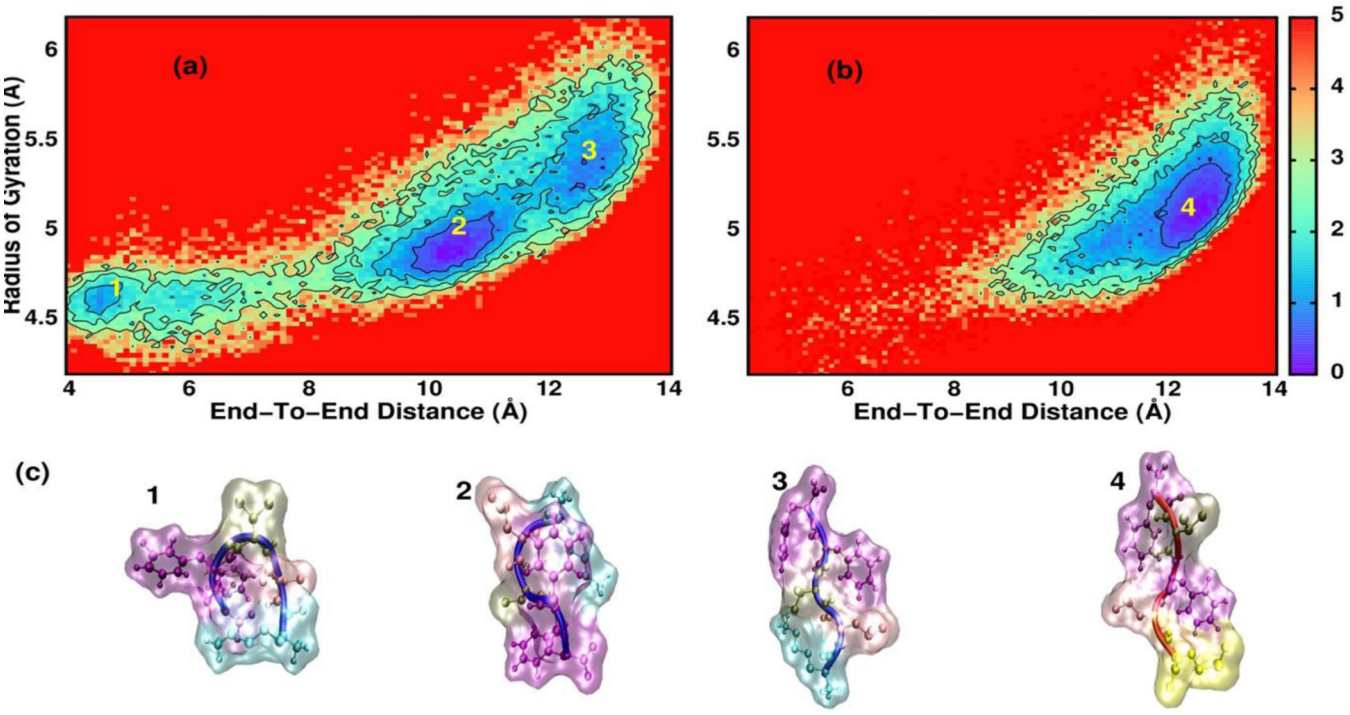

Figure 2.

Free energy landscape for monomer KLVFF (a) and FVFLM (b) as a function of radius of gyration and end-to-end distance.Surfaces are shown with contour lines indicating the relative 0.75kBT slope of the surface.(c) Shown are typical snapshots for local minima marked by 1, 2, 3 and 4.

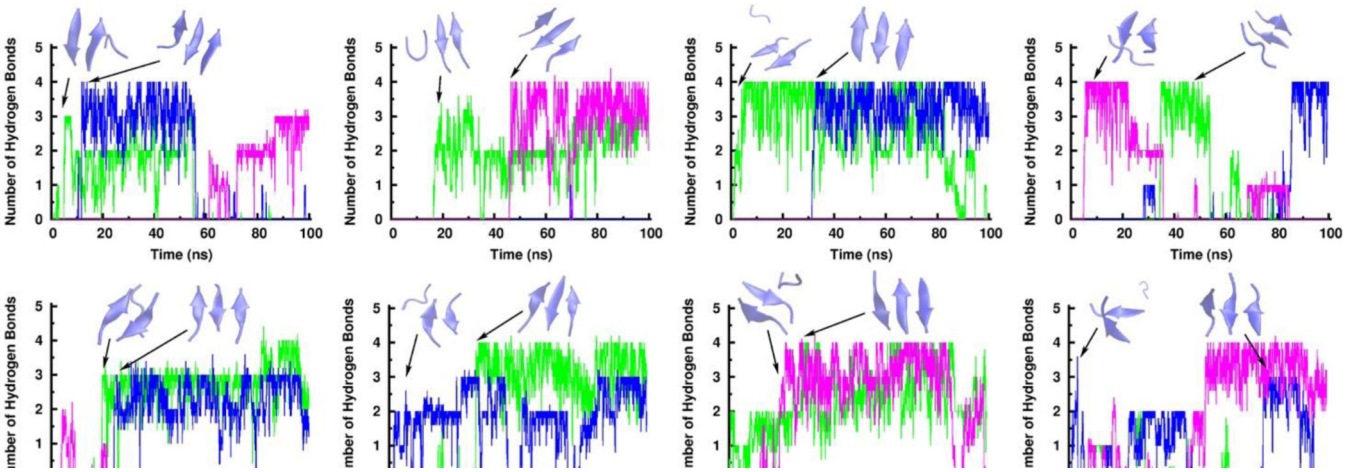

Figure 3.

Time dependence of the number of backbone hydrogen bonds between monomers FVFLM. Green, blue, and magenta curves represent the number of hydrogen bonds between peptide 1 and peptide 2, peptide 1 and peptide 3, peptide 2 and peptide 3, respectively.

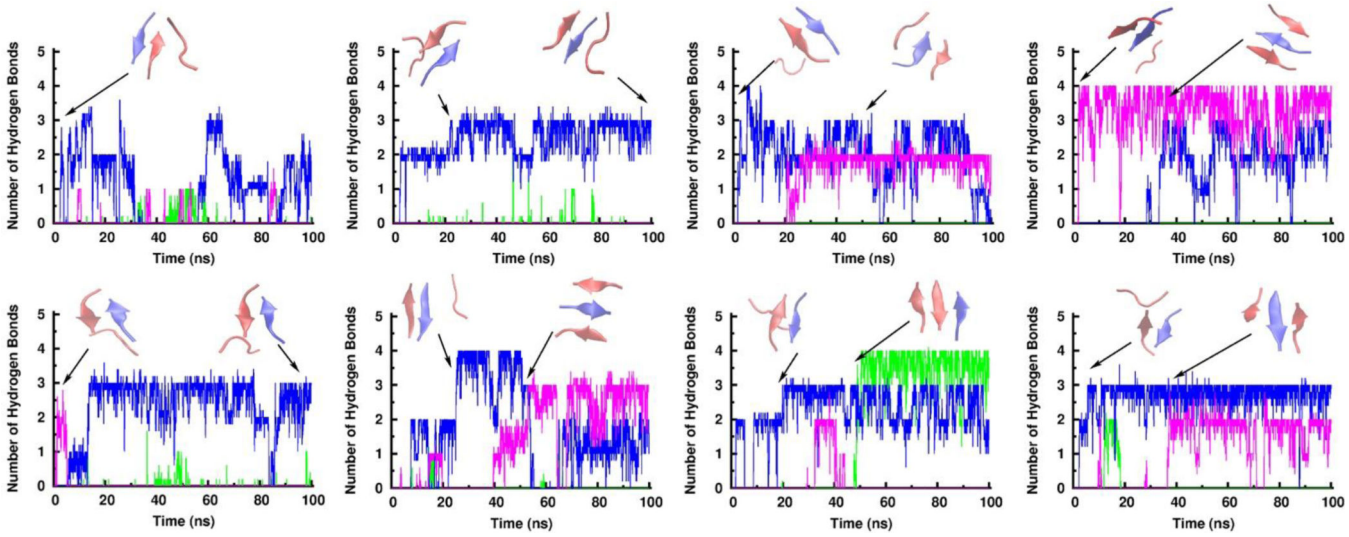

Figure 4.

Time dependence of the number of backbone hydrogen bonds between monomers. The green curve represents hydrogen bonds between Aβ16-20 peptides (KLVFF), while the blue and magenta ones show those between FVFLM andone of Aβ16-20 peptides (KLVFF). Snapshots showing FVFLM and $A\beta_{16–20}$ peptides are in blue and red colors, respectively.

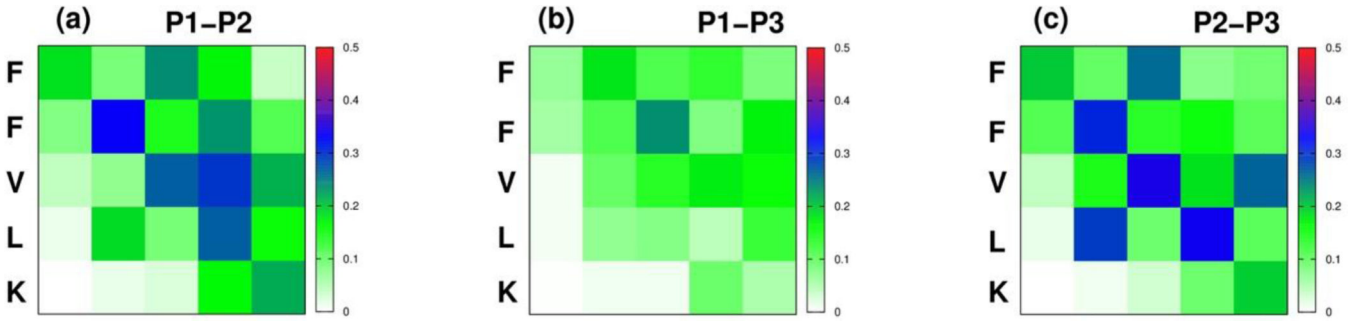

Figure 5.

Probability of side-chain contacts formation for the KLVFF trimer between peptide 1 (P1) and peptide (2) (a), peptide 1 (P1) and peptide (3) (b), peptide 2 (P2) and peptide (3) (P3) (c). Color bar showing the probability of SC appearance.

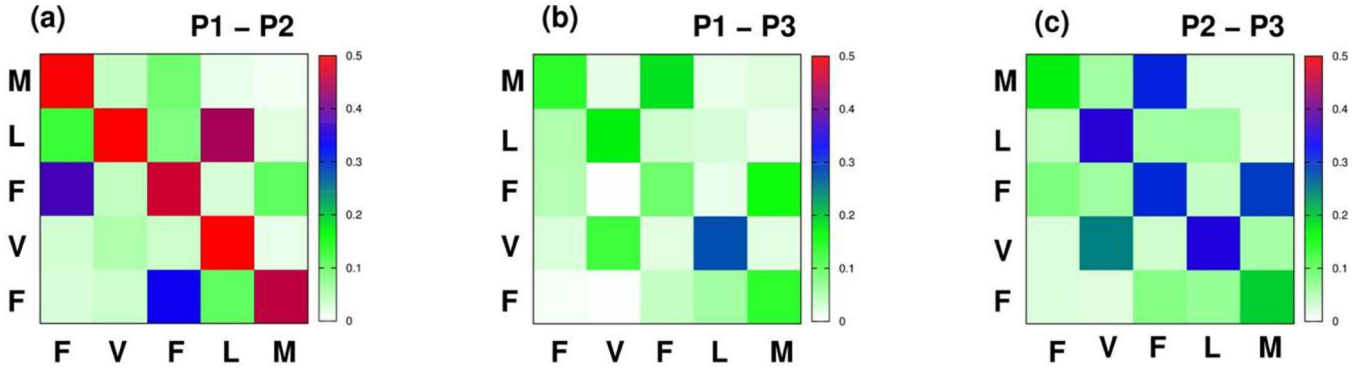

Figure 6.
Same as in Fig. 5, but for the FVFLM trimer